Subaquatic slope instabilities: The aftermath of river correction and artificial dumps in Lake Biel (Switzerland) — Source link

Nathalie Dubois, Nathalie Dubois, Love Råman Vinnå, Love Råman Vinnå ...+8 more authors

Institutions: Swiss Federal Institute of Aquatic Science and Technology, ETH Zurich, École Polytechnique Fédérale de Lausanne, Oeschger Centre for Climate Change Research ...+1 more institutions

Published on: 01 Feb 2020 - Sedimentology (Wiley)

Topics: River engineering

Subaquatic slope instabilities: The aftermath of river correction and artificial dumps in Lake Biel (Switzerland)

Nathalie Dubois[1,2], Love Råman Vinnå [3,5], Marvin Rabold[1], Michael Hilbe[4], Flavio S. Anselmetti[4], Alfred Wüest[3,5], Laetitia Meuriot[1], Alice Jeannet[6,7], Stéphanie Girardclos[6,7]

[1] Eawag, Swiss Federal Institute of Aquatic Science and Technology, Department of Surface Waters – Research and Management, Dübendorf, Switzerland

[2] Department of Earth Sciences, ETHZ, Zürich, Switzerland

[3] Physics of Aquatic Systems Laboratory, Margaretha Kamprad Chair, École Polytechnique Fédérale de Lausanne, Institute of Environmental Engineering, Lausanne, Switzerland

[4] Institute of Geological Sciences and Oeschger Centre for Climate Change Research, University of Bern, Bern, Switzerland

[5] Eawag, Swiss Federal Institute of Aquatic Science and Technology, Department of Surface Waters - Research and Management, Kastanienbaum, Switzerland

[6] Department of Earth Sciences, University of Geneva, Geneva, Switzerland

[7] Institute for Environmental Sciences, University of Geneva, Geneva, Switzerland

Corresponding author: Nathalie Dubois, Nathalie.dubois@eawag.ch

Associate Editor – Fabrizio Felletti

Short Title – Mass transport events linked to river correction

This document is the accepted manuscript version of the following article:

Dubois, N., Råman Vinnå, L., Rabold, M., Hilbe, M., Anselmetti, F. S., Wüest, A., … Girardclos, S. (2019). Subaquatic slope instabilities: the aftermath of river correction and artificial dumps in Lake Biel (Switzerland). Sedimentology. https://doi.org/10.1111/sed.12669

ABSTRACT

River engineering projects are developing rapidly across the globe, drastically modifying water courses and sediment transfer. Investigations of the impact of engineering works focuses usually on short-term impacts, thus a longer-term perspective is still missing on the effects that such projects have. The 'Jura Water Corrections' – the largest river engineering project ever undertaken in Switzerland – radically modified the hydrological system of Lake Biel in the 19th and 20th Century. The deviation of the Aare River into Lake Biel more than 140 years ago, in 1878, thus represents an ideal case study to investigate the long-term sedimentological impacts of such large-scale river rerouting. Sediment cores, along with new high-resolution bathymetric and seismic reflection datasets were acquired in Lake Biel to document the consequences of the Jura Water Corrections on the sedimentation history of Lake Biel. Numerous subaquatic mass transport structures were detected on all the slopes of the lake. Notably, a relatively large mass transport complex (0.86 km^2) was observed on the eastern shore, along the flow path of the Aare. The large amount of sediment delivered by the Aare River since its deviation into the lake likely caused sediment overloading resulting in subaquatic mass transport. Alternatively, the dumping since 1963 in a subaquatic landfill of material excavated during the second phase of river engineering, when the channels flowing into and out of Lake Biel were widened and deepened, might have triggered the largest mass transport, dated to 1964–1965. Additional potential triggers include two nearby small earthquakes in 1964 and 1965 (M_W 3.9 and 3.2, respectively). The data for this study indicates that relatively large mass transports have become recurrent in Lake Biel following the deviation of the Aare River, thus modifying hazard frequency for the neighbouring communities and infrastructures.

Keywords: High-resolution bathymetry, lake sedimentology, mass-transport deposits, river engineering, slope stability, subaquatic landfill.

INTRODUCTION

River engineering, dam construction and other human activities have drastically modified water courses and sediment transfer across the globe, with numerous additional constructions underway or planned. As a result, sediment transfer has changed in many places, either by direct sediment starvation (gravel and sand mining or sediment entrapment in reservoirs; Vörösmarty et al., 2003; Syvitski et al., 2005) or indirectly by flow modification reducing sediment transfer capacity (Gabbud & Lane, 2016). In Switzerland, several large-scale engineering projects had already modified watercourses two centuries ago, allowing the study of the longer-term sedimentological effects of such man-made modifications (e.g. Wirth et al., 2011).

Lake Biel, a Swiss Plateau lake on the foothills of the Jura Mountains (Fig. 1), is an ideal site to study the effects of river engineering on lake sedimentation. The Aare River was rerouted into Lake Biel at the end of the 19th Century as part of the large-scale 'Jura Water Corrections' (hereafter termed 'JWC'; Nast 2006). The first JWC, engineered from 1868 to 1891 in order to reduce flooding of the region, represents the greatest river management works ever undertaken in Switzerland. The Aare River deviation increased the catchment area of Lake Biel by a factor of 3.6 (Fig. 1), leading to a significant increase in sediment delivery from the catchment. This rerouting also increased the average water inflow from 55 to 240 m^3/s, which in turn reduced the mean residence time from 253 down to 58 days (Liechti, 1994).

This paper presents the results of a recent geophysical and sedimentological survey of Lake Biel. Multibeam bathymetry and reflection seismic data as well as sediment cores were acquired to study the major anthropogenic modifications of Lake Biel's sedimentary system. The key question to be addressed is: *what are the long-term consequences of the rerouting of the Aare River on the sedimentation in Lake Biel?*

STUDY AREA

Lake Biel [German: Bielersee, 47°5'N, 7°10'E, 429 m above sea level (a.s.l.), 39.9 km^2 surface area] is a perialpine lowland lake located between the Alps and the Jura Mountains in north-western Switzerland (Fig. 1), in a region commonly called 'Seeland' (literally 'Land of the Lakes') due to the presence of three lakes (Lake Biel, Lake Neuchâtel and Lake Murten). As part of the Swiss Plateau, the Seeland was shaped through former glaciations depositing extensive glacial till beds, but also eroding numerous glacial overdeepenings into the bedrock (Preusser et al., 2010). One of these overdeepened basins contains Lake Biel and Lake Neuchâtel, while a second one further south-east includes Lake Murten and the alluvial plain of the Aare River (Wolfarth & Schneider, 1991). The southern shore of Lake Biel is composed of Palaeogene to Neogene Molasse bedrocks forming relatively flat banks (Brombacher, 1997). The north shore of the lake has relatively steep banks caused by dipping Mesozoic strata, which are part of the southern edge of the Jura Mountains climbing to 1600 m a.s.l. in a distance of only 8 km. Due to its topography, the northern shore is only covered in certain places by a narrow alluvial zone (Brombacher, 1997).

Lake Biel is relatively shallow with an average depth of 31 m and a volume of 1.24 km^3 (Fig. 2). It comprises three major basins: the Tüscherz Basin (74 m maximum depth) in the north-east; the Lüscherz Basin (55 m) to the south of the 'St.

Petersinsel' peninsula; and the Neuenstadt Basin (35 m) to the north of the peninsula (Fig. 2). Lake Biel is warm monomictic and has changed from mesotrophic in the 1950s to eutrophic in the 1970s and is now meso-eutrophic (Wright et al., 1980; Liechti, 1994). Limnological characteristics are similar to those of other Swiss Plateau lakes. During the warm period (April to October), temperature increases in the upper layers and a stable density stratification develops. In winter (November to January), deep mixing of the lake results in a nearly homogenous water column and oxygen saturation is almost complete (Santschi & Schindler, 1977).

The main tributaries include the Thielle River, which forms the outlet from the nearby Lake Neuchâtel to the south-west, the Schüss River, which enters the lake in the city of Biel, and the Aare River, the only tributary to the southern basin and the main water supply of Lake Biel (Fig. 1C). The Aare River has only been flowing into Lake Biel since 1878 when as part of the first JWC framework it was diverted through the Hagneck Channel into the lake in order to control devastating floods in the surrounding Seeland area. It now supplies *ca* 80% of the water, suspended particulate matter and dissolved substances to Lake Biel (Santschi & Schindler, 1977). As the Aare River flows through Lake Brienz, Lake Thun (Fig. 1B) and the Wohlensee Reservoir (Fig. 1C) before reaching Lake Biel, most of Aare’s sediment is trapped in these upstream lakes (Wright et al., 1980; Thevenon et al., 2013). As a result, the sediment load carried by the Aare at the inflow at Hagneck largely derives from the Saane River, a major tributary that joins the Aare River 30 km upstream of Hagneck. Today, Lake Biel has a very large catchment area relative to the lake volume. Its drainage basin encompasses 8305 km^2 (about 20% of Switzerland), including large sections of the northern Swiss Alps, which creates a hydrological regime dominated by late spring snowmelt. The present-day hydrology of the lake differs greatly from that prior to 1878.

Early current measurements suggested that the water-circulation patterns in Lake Biel are strongly dominated by inflow-induced currents, setting up a general counterclockwise water circulation due to the deflection of the inflowing Aare to the right by the Coriolis force (Nydegger, 1967; 1976). In contrast, Albrecht et al. (1999) observed signatures of the plume flowing into the center of the lake. Using a hydrodynamic approach, Råman Vinnå et al. (2017a) recently explained the existence of those two characteristic patterns by a wind-induced lake circulation. North-easterly winds and resulting clockwise lake circulation will move the plume toward the lake center while south-westerly winds will push the plume counterclockwise towards the south-east shore. The composition of the surface sediment reflects this circulation pattern, with terrigenous Aare River material predominantly deposited along the south-east shore and in the Tüscherz Basin, to the right of the river mouth (Weiss, 1977; Wright & Nydegger, 1980). Sedimentation in the Neuenstadt Basin is influenced by particles from the Thielle Channel, which may explain the higher sedimentation rate relative to that in the Lüscherz Basin (Wright et al., 1980).

Hydropower plants have also changed the flow of water and particles in the upstream Aare system. Upstream of Lake Brienz, the flow of the Aare River is affected by seven reservoirs associated with hydropower units. These hydropower dams in the high-Alpine Grimsel area (constructed in the 1930s to 1950s) have altered the seasonality of the Aare River flow (shift of some of the particle input from summer to winter) and reduced the particle input from upstream glaciers to Lake Brienz by two-thirds (Wüest et al., 2007; Anselmetti et al., 2007). The most important hydrological change in the Saane River system (Fig. 1) was the construction of the Rossens Dam in 1948 (Fig. 1C). Since then, the Saane River discharge pattern has been heavily influenced by hydroelectricity production, which maintains the downstream water discharge almost constant, excluding times of strong flood events (Thevenon et al., 2013). Since 2016, artificial floods are being tested on the Saane River to recreate the natural rhythm of the river and eliminate the negative impacts of the hydropower plant, such as algae growth, clogging sediments, and species that have moved in profiting from the unnatural flows (Cook, 2017).

The construction of the Hagneck hydropower plants on the mouth of the Hagneck Channel in 1900 (Nast, 2006) reduced the energy level and, therefore, the sediment transport capacity of the Aare River. Following critical floods in 2005 and 2007 and an imminent dam collapse in 2007, the Hagneck Channel was renovated for the first time after 130 years. Between 2010 and 2015, side dams were raised and widened, and slopes stabilized to resist discharges up to 1500 m^3/s (i.e. a 100 year flood). The Hagneck hydropower plant was also rebuilt, raising the electricity production from 11 MW to 24 MW (Amt für Wasser & Abfall, 2015).

THE JURA WATER CORRECTIONS

Starting from the Middle Ages, numerous historical records describe catastrophic flood events in the Seeland region surrounding the lakes of Neuchâtel, Murten and Biel. First mention of these events is made with reference to a ‘millennial flood’ in 1342, which was followed by several other damaging floods (Nast, 2006). Obviously, not all flood events were reported but, based on written testimony, Nast (2006) inferred that major Seeland floods occurred on average every 9.5 years between 1500 and 1882. As a result of these floods, the Seeland was a poverty-stricken marshy area in which the risk of epidemics such as malaria was very high, and agriculture and farming were difficult.

The first documented flood mitigation measures were taken in the second half of the 16th Century: fish traps were banned from the Thielle River (flowing out of Lake Biel, now the Nidau–Büren Channel, Fig. 1) in Nidau, in order to avoid any blockage of the outflow (Vischer, 2003). However, flooding remained recurrent. The worst historic flood was recorded in 1651, when the overflowing Aare River merged with Lake Biel to form one large 'Lake of Solothurn', spreading from the lake to the City of Solothurn (location in Fig. 1; Schneider, 1881; Vischer, 2003). Additional measures were then implemented to prevent such catastrophic floods, and several regional projects were initiated, marking the beginning of the Jura Water Corrections era.

In 1868, after multiple debates about the planning and the realization of the river engineering, the cantons of Bern, Fribourg, Vaud, Neuchâtel and Solothurn finally launched the first major modification of the hydrological system of the Seeland and neighbouring regions: the first JWC. One of the major achievements of this project was the construction of an 8 km long deviation channel, the Hagneck Channel. As a flood control scheme, the path of the Aare River was modified downstream of Aarberg to flow directly into Lake Biel (Fig. 1; Nast, 2006). The construction of the Hagneck Channel involved the excavation of millions cubic metres of Molasse bedrock, composed of hard sandstones and alterable marls (Vischer, 2003). Before the opening of the Hagneck Channel in 1878, the Thielle River (lake outlet) had to be widened. The JWC thus started in 1868 with the construction of the Nidau–Büren Channel, which led to a rapid lake level drop (2 m). The construction of the Hagneck Channel then started in 1873, and the channel was opened in 1878, but the river continued to intensely erode the riverbed in the channel due to the changed gradient along the river and new stabilization constructions were built between 1887 and 1900

(Thevenon et al., 2013). With the completion of these additional constructions, the Hagneck hydropower plant was finally inaugurated in 1900 (Nast, 2006). In addition to this major deviation, the regional river management program also included the channelization of the naturally inflowing small rivers Broye and Thielle, which started in 1874 and 1875, respectively. The JWC, especially the lowering of the mean lake level by 2 m, allowed drainage of the surrounding wetland areas. The formerly swampy Seeland became a vast fertile agricultural area. Changes in the soil and surface properties following this major landscape and river managing work even affected the local and regional climate on the Swiss Plateau (Schneider et al., 2004).

A second phase of river engineering took place between 1962 and 1973: the second JWC. The need for this second phase had already been anticipated at the time of the first JWC. It consisted essentially of the construction of the Flumenthal Dam in 1970, *ca* 20 km downstream of Lake Biel (Fig. 1), to regulate the outflow of the three-lake hydrological system and the confluence with the Emme River. In addition, the Broye (1962 to 1970), Thielle (1965 to 1970) and Nidau–Büren (1963 to 1973) channels were widened and deepened, each by a few metres (Fig. 1). An estimated 2.7 million cubic metres were excavated from the Nidau–Büren Channel and dumped with hopper barges into a subaquatic disposal site in Lake Biel, between Ipsach and Sutz–Lattrigen (Chavaz & Gygax, 1964). The hopper barges were emptied in a water depth of *ca* 10 m in order to reduce turbidity at the lake surface, and at the top of the slope so that the material would slowly make its way down to deeper grounds (Josef Frommelt, 2nd JWC hopper barge pilot, Schlossmuseum Nidau). The emptying lane was delimited with buoys and moved stepwise every week. For some of the material, however, such as lake chalk, the barges had to navigate 3 to 4 hours in the middle of the lake to be able to rinse it out using a water hose. Since the second JWC, only two major floods have occurred in the Seeland, in 2007 and 2015.

PREVIOUS INVESTIGATIONS

Jeannet (2012) investigated a 10 m long composite percussion piston core recovered close to the Aare River mouth in the Lüscherz Basin (black star in Fig. 2), in an effort to detect changes in sediment composition following the first JWC. The core was retrieved using an ETH Zurich/Eawag Uwitec system. In order to minimize the sediment loss and/or sediment disturbances induced by the coring technique, two long cores BIE11-1 and BIE11-2 were taken on contiguous sites with a 0.5 m overlapping in depth (Suppl. Mat.).

The main findings are summarized hereafter. The deviation of the Aare River is evidenced by changes in the grain-size distribution, in the sedimentation rate and in the elemental composition. Major/minor element distributions from X-ray fluorescence (XRF) core-scanning reveal an abrupt increase in elements of allochthonous origin (Ti, Si, K, Fe and Mn) in response to the Aare River deviation, while Ca decreases. Higher Fe/Mn ratios suggest an increase in oxygen supply to the hypolimnion subsequent to the new permanent inflow of large water masses. The sediments deposited during the years following the end of the Hagneck Channel excavation display significantly coarser material (144.5 to 147.5 cm depth, 1878 AD; >60 vol % of sand-size particles), which clearly reveals an event of strong water discharge flowing into the lake, intense enough to erode and transport such coarse grains. The sedimentation rates subsequently stabilized at *ca* 0.89 cm/yr (Suppl. Mat.), six times higher than before the Aare deviation (*ca* 0.15 cm/yr for the last 6000 years).

METHODS

Bathymetry data

In March 2015, a high-resolution bathymetric dataset was acquired with a multibeam echosounder (Kongsberg EM2040; 1° × 1° beam width; operating at 300 kHz; Kongsberg Maritime, Kongsberg, Norway), installed on the *R/V ArETHuse*. A more detailed description of the method and the used equipment has been published by Wessels et al. (2015); thus only a brief summary is provided hereafter. Positioning of the survey vessel was done with a GPS/GNSS receiver (Leica GX1230+ GNSS; Leica Geosystems AG, St Gallen, Switzerland) in combination with the RTK positioning service 'swiposGIS/GEO' streamed from a mobile communications network, providing centimetre-level accuracy. Attitude and heading of the vessel were monitored with a Kongsberg Seatex MRU5+ inertial navigation system and a Trimble SPS361 GPS compass (Trimble Inc., Sunnyvale, CA, USA), respectively. Data were recorded with the Kongsberg SIS software. Sound-velocity profiles in the water column for depth calculation were acquired several times per day with a Valeport miniSVP probe (Valeport Limited, Totnes, UK). Raw data were processed with CARIS HIPS/SIPS 9 (Teledyne CARIS Inc., Fredericton, NB, Canada). From the cleaned point cloud, a gridded dataset with 1 m cell size was generated, providing the elevation of the lake floor. The shallow (<5 m water depth) nearshore zone cannot be measured efficiently with this multibeam technology and was instead measured using airborne topobathymetric laser scanning (LiDAR). Wessels et al. (2015) provide more details on the applied LiDAR methodology. The two datasets (multibeam and LiDAR data) were subsequently merged in order to obtain a seamless digital terrain model (DTM) of the entire Lake Biel (Fig. 2). Analyses, descriptions and interpretations of the bathymetry were performed in standard GIS software and are mainly based on shaded reliefs of the dataset.

Reflection seismic data

A total of 45 km of reflection seismic profiles were acquired on 26 April 2010 using a single-channel 3.5 kHz pinger source fixed on an inflatable cataraft that was pushed in front of the *R/V ArETHuse*. The seismic profiles were recorded digitally in SEG-Y format, using GPS (error ± 5 m) for navigation. Seismic data were processed using band-pass filtering (2.2 to 6.3 kHz). The time–depth conversion in water and sediment is based on a constant P-wave velocity of 1450 m/s. Vertical seismic resolution is defined as one quarter of the wave length of the seismic signal (Rayleigh, 1885) thus *ca* 10 cm for the 3.5 kHz source. Interpretation of seismic data was accomplished with the KingdomSuite™ 8.1 software.

Sediment coring and analyses

Forty-eight short cores of 1 to 2 m in length and 63 mm in diameter were retrieved with a gravity corer (Eawag-63/S corer; Eawag, Dübendorf, Switzerland). Campaigns took place in 2010, 2013, 2014, and in 2015, after the bathymetry campaign. Sixteen cores were logged using a GEOTEK multi-sensor core logger (Geotek Limited, Daventry, UK): Gamma-attenuation bulk density, P-wave velocity, and magnetic susceptibility were measured at intervals of 0.5 cm. All cores were split for further description and analyses. Open cores were photographed using a line scan camera.

Elemental analysis of five sediment cores was performed with an Avaatech X-Ray Fluorescence (XRF) core-scanner (Avaatech XRF Technology, Dodewaard, The Netherlands) with resolutions of 1 cm for four cores (BIE 14-54, BIE 14-58, BIE 14-

59 and BIE 14-60) and 2 mm for one core (BIE 14-52). Grain size in the range of 0.02 to 2000 µm was measured for seven cores using laser-diffraction technique (Malvern Mastersizer 2000; Malvern Panalytical, Malvern, UK). Samples were dispersed in Calgon® (Sodium Polymetaphosphate) prior to analysis and disaggregated by ultra-sonication. Each sample was measured at least three times. Samples were analysed for grain-size distribution at 1 cm resolution in cores BIE-14-52 (from 0 to 88 cm) and BIE-14-61 (from 0 to 111 cm), whereas 10 discrete samples were analyzed in cores BIE-14-54, BIE-14-57, BIE-14-58, BIE-14-59 and BIE-14-60. The core logging, XRF core-scanning and grain-size analyses were performed at the Limnogeology Laboratory of ETH Zurich.

Aliquots of the same sediment samples analyzed for grain size were freeze-dried and ground to quantify their total carbon (TC) content using an Elemental Analyzer EURO EA 3000 (EuroVector SpA, Milan, Italy) and their total inorganic carbon (TIC) content using a CM5015 Total Inorganic Carbon Analyzer (UIC Inc., Joliet, IL, USA). Both measurements were conducted at the Sedimentology Laboratory at Eawag. The total organic carbon (TOC) content was derived from TOC = TC – TIC.

The 137-Caesium (^{137}Cs) activity in the samples of cores BIE10-9, BIE-14-61 and BL13-1C was determined on high-purity Germanium Well Detectors (Canberra Industries) at the Gamma Laboratory at Eawag. A total of 5 to 10 g of freeze-dried and ground sediment samples was weighted into sample tubes.

RESULTS

Multibeam

Because the layout and general topography of the basins have been known since the first bathymetric surveys, this study focuses on distinct geomorphological features revealed by the high-resolution bathymetric data. Features characteristic of subaqueous mass transports are evident on the lake bed. Interpretation and mapping of these features rely on descriptions of the morphology (escarpments, head scars, bulges and ridges), but also on the identification of surface textures, i.e. small-scale relief resulting in a distinct appearance of the lake floor in hillshade images (Fig. 2).

Mass transport structures

Numerous subaquatic mass transport structures are clearly distinguishable in the lake bottom topography, both on the north-western slope, which is characterized by steep slopes (up to *ca* 30°), and on the more gently dipping south-eastern slopes. The Lüscherz Basin, at the south-western end of the lake, hosts 18 mass transport structures. On the north-western slope of the main Tüscherz Basin, mass transport structures cover rather small areas (0.02 to 0.3 km^2; Figs 2 and 3A). In the region Ligerz–Twann, only five such mass transport structures can be observed, while eight mass transport structures are visible in the region Tüscherz–Alfermée, some of them with erosional channels incising the north-western slope (Fig. 3B). On the south-eastern slopes of the Tüscherz Basin, mass transport structures are less numerous, but they form a mass transport complex covering a total surface of 0.86 km^2 (Fig. 4). The amalgamated headwall extends laterally over 1 km at the upper slope break in *ca* 5 m water depth. This relatively large mass transport complex is visible between Sutz–Lattrigen and Ipsach. Four distinct compartments can be distinguished based on the geometry of the headwall and frontal lobes that are identified with four different colours (black, yellow, orange and red; Fig. 4). Ridges in the headwall clearly separate the red from the orange mass transport deposit (MTD) and the orange from the yellow MTD. Different topographies/roughness of the sediment surface in the four

MTDs suggest the amalgamation of mass transports of different ages (Figs 2 and 4). Based on overprinting relations (black over yellow, orange over yellow) and the gradient in surface topography/roughness (red > orange > yellow), the relative timing of the mass transport occurrences was preliminarily deduced as: (i) yellow; (ii) black; (iii) orange; and (iv) red. The surface topography of the black MTD was not directly compared with the three larger ones, as its extent is more limited and its headscar (i.e. the source and transit areas of the mass transport) is located towards the bottom of the slope possibly influencing the surface texture. Similarly, the headscar of the red mass transport is located slightly below the slope break, whereas the yellow and orange MTDs originated from the slope break. The higher topography of the red MTD could thus also be the result of a different type of mass transport.

The headscars are bounded by sharp escarpments at the upper slope break, bordering the shore platform. The MTDs in deep Lake Biel form irregular packages, typical for deposits that have been transported in a rather coherent way over a limited distance. Additionally, the surface structure of the MTDs at the foot of the slope, in particular their pronounced relief (elongated ridges of a typical height of 1 to 2 m, separated by 5 to 20 m), suggests that large portions moved as coherent packages. Similar structures have also been explained by in-place deformation of basin sediments (Schnellmann et al., 2005). The adjacent slope to the north-east of the mass transport complex reveals rippled surface that we attribute to creeping (Fig. 4), a common phenomenon in gas-rich sediments (Ledoux et al., 2010).

Pockmarks

In addition to numerous mass transport structures, the lake floor morphology is characterized by almost a dozen rounded depressions of varying sizes: most are approximately 20 to 30 m in diameter, while the two larger ones are approximately 60 to 70 m in diameter (Fig. 3C). These depressions are interpreted as pockmarks. Seven pockmarks are located at the foot of the slopes along the north-western shore close to the Jura Mountain front, between Ligerz and Twann (Fig. 2), in a similar position as the giant pockmarks discovered in Lake Neuchâtel (Reusch et al., 2015). However, three pockmarks are located at the foot of the southern slope of the St. Petersinsel, almost in the central part of the Lüscherz Basin (Fig. 2). In both locations, some of the pockmarks reveal a succession of pockmarks of different sizes and ages, the older stages appearing less sharp (Fig. 3C). The pockmarks of Lake Neuchâtel were interpreted as caused by groundwater seepage sites, where groundwater from the Jura Mountain karst system flows into the lake (Reusch et al., 2015). As the pockmarks between Ligerz and Twann are located in a similar position on the foot of the Jura slope, their formation is probably very similar to those of Lake Neuchâtel. Similar groundwater discharge could be causing the pockmarks in the Lüscherz Basin, although gas seepage cannot be excluded as a formation mechanism, given the high gas content of Lake Biel sediments (see gas blanking in the *Seismic stratigraphy* section below). In nearby Lake Le Bourget, a series of collapse craters (20 to 30 m diameter) were identified near the incipient scars of an ongoing large sublacustrine sediment slide (Chapron et al., 2004; Ledoux et al., 2010). These collapse craters were interpreted as resulting from the expulsion of water and/or gas migration due to faults in the sediment, and to sediment liquefaction induced by earthquakes or by the increasing pore-pressure due to sediment loading (Chapron et al., 2004). In Lake Biel, however, the pockmarks are not located close to subaquatic MTDs, and thus cannot be associated with them.

Sediment waves

The relatively wide south-eastern shore platform hosts numerous parallel elongated bedforms that stretch from the north-east to the south-west, especially in front of Gerolfingen (Figs 2 and 3D). These bedforms are slightly curved to almost straight sediment waves with typical wavelengths of several tens of metres, along-crest lengths of up to 500 m and heights of a few decimetres. They are often asymmetrical, with a steeper slope towards the convex south-eastern side and typical slope angles of 1.5 to 6.0° on the short side and 0.5 to 3.0° on the long side. Because neither indications of their migration direction, nor data on their sediment grain size or internal structure are available, no interpretation as to whether they may represent dunes, antidunes or cyclic steps (Cartigny et al, 2011; Covault et al., 2017, Symons et al, 2016) is given. However, the fact that the water depth in which these features occur is only around 2 to 6 m makes it likely that these sediment waves are linked to coastal currents induced by wind waves.

Seismic stratigraphy

Due to high methane content in the sediments (gas blanking), the seismic signal did not penetrate deep enough to image the deep sedimentary units. However, the structure of the sediment surface (i.e. the lake floor) as well as shallow units down to almost 1.5 m (i.e. 2 ms in two-way travel time – TWT) can be distinguished (Fig. 5). On the seismic profile along the lake's axis (hereafter longitudinal line) and on several transverse lines, the lake floor appears disturbed (rough irregular surface) over a quite large area (*ca* 0.5 km^2). There, the uppermost sediments reveal acoustically semi-transparent to chaotic deposits, clearly identified as mass transport structures on the multibeam bathymetry. Interestingly, on transverse line T2 (Fig. 5E), the lake bottom surface topography appears more irregular (i.e. 'rougher') than on transverse line T3 (Fig. 5D). As described in the *Mass transport structures* section, a gradient in surface topography was also visible in the multibeam bathymetry across the MTD complex (Fig. 4). Strupler et al. (2015) clearly showed the relationship between the surface roughness of the translation area and the age of various prehistoric and historic slides in Lake Zurich, Switzerland. The 'roughness' of the surface of the MTD crossed by T2 thus suggests that this mass transport structure is more recent than the one crossed by T3.

On the longitudinal line, a seismic unit with low reflection amplitudes (almost transparent) can be traced across the Tüscherz Basin, with increasing thickness towards the deeper basin (Fig. 5A to C). This seismic unit reaches *ca* 35 cm thickness (0.5 ms TWT), thus is above the limit of vertical seismic resolution (*ca* 10 cm). It is located in-between seismic units of higher amplitudes showing undisturbed layered sediments, the topmost being the lake-floor reflection.

Sediment cores

Only the sediment cores most useful for the interpretation of mass transport and sedimentary units (n = 20) are presented. Undisturbed Lake Biel sediments, as retrieved in the basin outside the MTD (cores BIE10-9, BL13-1C, BIE-14-60, BIE-14-61, BIE-14-62, BIE-14-88, BIE-14-92, BIE-14-93, BIE-14-95; Figs 4 and 6), have a greyish to brownish colour, are moderately layered, with an organic carbon content of *ca* 2 wt% and an average calcium carbonate content of 32 wt%. The average grain-size distribution is 10 to 20% clay, 60 to 80% silt and *ca* 5% sand. The upper 1 to 2 cm usually reveal an oxidized (yellowish) layer. Three cores (BIE-14-92, BIE-14-93 and BIE-14-88) located outside but close to the MTD complex reveal an alternation of

1 to 2 cm thick light grey and dark beige layers between 60 cm and 85 cm depth (Fig. 6). At the same depths, several cores reveal a small (<1 cm) layer of lake chalk (whitish colour; BIE-14-60, BIE-14-81, BIE-14-82, BIE-14-83, BIE-14-92, BIE-14-93, BIE-14-95; BIE-15-06 and BIE-15-06-08; Fig. 6).

Cores located in the central basin reveal one or sometimes two beds interpreted as turbidites: an up to 13 cm thick dark beige homogenous layer centred around 20 to 30 cm depth and an up to 4 cm thick light grey homogenous layer located between 65 cm and 85 cm depth depending on the core [cores BIE10-9, BL13-1C, BIE-14-59, BIE-14-61, BIE-14-62, BIE-14-88 and BIE-14-95, underlined (Fig. 4) or bracketed (Fig. 6) in green].

Core BIE-14-60 at the base of the slope contains a 20 cm thick layer of dark sand (11 to 33 cm depth), which can be correlated to the upper dark beige turbidite (Fig. 6). In addition to the thick deposit in BIE-14-60, several cores located in the basin (BIE-14-58, BIE-14-81 and BIE-14-92) and on the slope (BIE-14-57) reveal a small 0.5 to 1.0 cm layer of dark sand around 11 cm sediment depth (Figs 4 and 6). The fact that this sandy layer is located in every core at a depth of *ca* 11 cm points towards a single event causing this deposition, and not, for instance, sand from the dunes on the south-eastern shore platform sliding downslope, as this would occur multiple times. Since this sand layer is present in cores across the yellow MTD and outside the MTD complex, it does not reflect the deposit resulting from one of the mass transports in the complex. Interestingly, core BIE-14-77 located upslope reveals a sharp transition at 8 cm depth, from well-oxygenated beige silts to a base composed mostly of darker sand (Fig. 6). This sharp transition most likely represents a sliding surface, either of the yellow MTD and/or of the dark sand layer. The authors interpret this dark sand layer as the deposit of an upper slope failure of sandy units with geometries too small to be distinguished on the multibeam bathymetry.

Sediment cores retrieved from the yellow MTD reveal greyish to brownish moderately layered sediment down to *ca* 60 cm. The upper 60 cm can be relatively well correlated from core to core (Fig. 6), but such a correlation is nearly impossible for the deeper parts. At *ca* 60 cm, lake chalk appears (core BIE-14-81 and BIE-14-82) as well as sand lenses (BIE-14-59, BIE-14-81 and BIE-14-82) and mottled sediment (core BIE-14-81 60 to 63 cm, or BIE-14-58 below 60 cm). Mottled sediment is also present at similar depth in a nearby core outside the MTD (BIE-14-92 67 to 70 cm). This layer could potentially be linked to the black (or yellow) MTD, as core BIE-14-92 was retrieved just in front of it. However, since this deformed interval consists mainly of lake chalk, it cannot be ruled out that it was caused by the dumping of material (i.e. lake chalk) during the rinsing of the hopper barges.

The sediment cores from the orange MTD (BIE-14-54 and BIE-14-55) both reveal a distinct feature at *ca* 35 cm depth (Fig. 6): core BIE-14-55 is only 34 cm long, whereas core BIE-14-54 shows a clear shift at 35 cm depth, from well-layered beige-brown sediments on top to more greyish mottled sediment below. The transition is marked by coarser grain size. Additional layers of coarser grains can be seen throughout the mottled sediments. A second shift towards darker sediment can be observed at 63 cm, close to the bottom of the core (at 65 cm).

The sediment cores retrieved from the red MTD (BIE-15-06, BIE-15-07 and BIE-15-08) can be relatively well correlated with each other down to 50 cm (Fig. 6). In core BIE-15-06, the layers become more tilted between 10 cm and 40 cm. Whereas core BIE-15-07 only reaches 50 cm, both BIE-15-06 and BIE-15-08 reveal strange material below 60 cm, such as very light grey clays (BIE-15-06) and an angular stone, sand and mudclast (BIE-15-08), which can be clearly distinguished by their distinct colours and/or grain size (Fig. 6).

Dating the mass transports

Generally, mass transports can be best dated based on the accompanying turbidites deposited in the basin, where sedimentation is continuous and undisturbed. As discussed above, cores located in the deepest part of the Tüscherz Basin reveal only two large turbidites (green brackets, Fig. 6). The ^{137}Cs activities profile in cores BIE10-9 and BIE-14-61 (Fig. 7) allows precise dating of the two turbidites: 1964 to 1965 for the grey-coloured one and the year 2000 for the thick dark beige one. In addition to the 1963 nuclear bomb testing ^{137}Cs peak and the 1986 Chernobyl accident ^{137}Cs peak, the ^{137}Cs activities profile in Lake Biel sediment reveals several additional peaks, which were previously reported (Albrecht et al. 1998; Thevenon et al., 2013). The anomalous ^{137}Cs peaks dated to 1977 and 2000 were caused by radionuclide discharges from the upstream Mühleberg Nuclear Power Plant (NPP, Fig. 1). The smaller peaks in 1981 and 1983 were also detected by Albrecht et al. (1998, see Fig. 3F) and Thevenon et al. (2013, see Fig. 2), but not discussed in detail. Instead, Albrecht (1998) reported on a ^{60}Co activity peak related to higher wastewater discharges from the Mühleberg NPP documented in August of 1982, which can probably also explain the smaller ^{137}Cs peaks at that time.

The upper dark beige turbidite dated to the year 2000 has been correlated to the sand layer and therefore was not caused by one of the identified MTD (Fig. 6). The 1964 to 1965 turbidite in core BIE-14-61 (63 to 65 cm depth) can be correlated to the lowermost (*ca* 60 cm depth) undisturbed moderately layered sediment in nearby cores part of the yellow MTD (BIE-14-58, BIE-14-59 and BIE-14-81; Fig. 6). Therefore, it is suggested here that the 1964 to 1965 turbidite represents the basinal layers of the yellow MTD. The shift at *ca* 60 cm depth in cores BIE-14-58, BIE-14-59, BIE-14-81 and BIE-14-82 corresponds to the top of the yellow MTD, with the moderately layered sediment on top corresponding to post-event drape (Fig. 6). This yellow MTD has a smoother topography both on the multibeam and on the seismic line (T3; Figs 4 and 5), as it is covered by a sediment drape.

The three other MTDs (black, orange and red) are difficult to date precisely because they cannot be correlated to a turbidite. The small black MTD, which started mid-slope, overprints the yellow MTD and must thus be younger (Fig. 4). Given its proximity to the cores with the dark sand layer and the 2000 turbidite, the small black MTD may be linked to this 2000 sedimentological event. Unfortunately, core BIE-14-93, which is located on the edge of the black MTD, does not provide any hints to date this event (Fig. 6).

The orange MTD, on the other hand, reveals a rougher topography than the yellow MTD, both on the seismic (Fig. 2, T2) and on the multibeam data (Fig. 4). In addition, the multibeam bathymetry suggests some overprinting of the orange MTD on the north-eastern part of the yellow mid 1960s MTD (Fig. 4) indicating a younger age. Core BIE-14-54, retrieved within this MTD, reveals a shift at 35 cm from well-layered beige-brown sediments on top to more greyish mottled sediment below as well as a second shift at 63 cm. Core BIE-14-55, also within the spatial extent of orange MTD, does not penetrate below the upper shift. These shifts possibly indicate transitions between different sediment blocks of the MTD (yellow and orange stars, Fig. 6). The upper 35 cm in the two cores seem to reveal a well-layered post event drape. Based on 35 cm of post-event drape and an average sedimentation rate of 1.2 cm/yr obtained from the ^{137}Cs dating (Fig. 7), the orange MTD could thus be dated to the early 1980s. However, considering all uncertainties, its age remains speculative.

Interestingly, the event of the orange MTD did not produce any turbidite in the deeper Tüscherz Basin. The rougher topography might indicate that the orange MTD moved as a coherent package, pointing to a mass movement that probably did not disintegrate into a mass flow, which in turn would explain the absence of a large-scale resuspension of finer particles leading to an associated turbidite in the sediment record. Another explanation for the absence of turbidites associated to the orange MTD could be the higher topography due to the formerly deposited yellow MTD, which might have been able to stop the path of weak turbidity currents originating from the north-east during the orange mass transport event.

The red MTD in the north-eastern part of the MTD complex has the roughest topography (visible on the multibeam data, Fig. 4), possibly pointing to a very recent event. However, as suggested above, the rougher surface topography of the red MTD, which originated below the slope break and not at the slope edge like the orange and yellow MTDs, could also be the result of a different type of transport. A major argument in favour of this second interpretation is the absence of an MTD-related sediment facies in the upper part of the cores located in the red MTD (BIE-15-06, BIE-15-07 and BIE-15-08). In addition, the first 50 to 60 cm sediment intervals of these cores can be relatively well correlated to those of core BIE-14-82, located in the yellow MTD. Moreover, sediment cores within the red MTD reveal a clear shift or transition at 50/60 cm core depth (Fig. 6) with material consisting of very light grey clays (BIE-15-06), angular stone, sand and mudclast (BIE-15-08). As the transition to conspicuous material occurs at a similar core depth in both the red (50/60 cm) and the yellow MTD (*ca* 60 cm depth) and they both have the yellowish/whitish layers on top of the MTD, the red mass transport might have occurred at the same time as the yellow mass transport, thus in 1964 to 1965.

Interestingly, the lake intake pipe for the drinking water supply of the City of Biel, which is located at *ca* 40 m depth in the vicinity of Ipsach (Fig. 2, exact location cannot be disclosed for security reasons), reported a large turbidity event at 06:00 on 31 December 2009 (Energy Service Biel, personal communication; Råman Vinnå et al., 2017b). Analysis of lake-level recordings at Twann revealed an oscillating signal with a period of 30 min shortly before from 04:00 to 06:00 (Råman Vinnå, 2018). This type of signal is extremely rare in the records of that station. It is just within the spatial and temporal resolution of the instrument (1 mm and 10 min), but still resolvable despite the built-in wave damping. The classical interpretation for this event is that it was due to a small-scale shallow water wave (tsunami or seiche), itself likely caused by an underwater mass transport event that produced the associated water turbidity. The initial interpretation of this study, based solely on multibeam data, was favouring the close-by red MTD as the potential source and cause for the 31 December 2009 turbidity event. However, the sediment record data herein is not pointing towards such a hypothesis because it would require a very recent trace in the sediment record, which was not observed. In addition, the authors would tend to exclude smaller scale mudflows coming from the north-western shore as possible sources for this large turbidity event because they could not have caused the observed small-scale shallow water wave. At this stage, the cause of the 31 December 2009 event thus remains a scientific mystery.

DISCUSSION: POTENTIAL CAUSES OF THE RECENT LAKE BIEL SUBAQUATIC INSTABILITIES

The subaqueous landscape of Lake Biel reveals numerous mass transport structures that happened on relatively gentle slopes. The occurrence of such mass transports is well-known in high-seismicity context (Moernaut et al., 2014; Praet et al., 2017) but the Lake Biel area is not particularly seismic, as no earthquake above M_W 4 and only 11 earthquakes above M_W 3 occurred during the last 100 years in a 20 km radius around the lake (Fäh et al., 2011). At the time of the initial failure of the mass transport complex, only two small earthquakes happened near Lake Biel with a magnitude of 3.9 and 3.2, in 1964 and 1965, respectively (Fäh et al., 2011). The 1964 event was located between Courgevaux and Coussiberlé at 46.9°N, 7.117°E (*ca* 23 km away from the slide), whereas the 1965 earthquake occurred at 47.0°N, 7.2°E by Fräschels (*ca* 11 km away from the slide, see Fig. 1 for location of the epicentres). Previous work in Swiss lakes showed that deformation structures start to form in sediment during ground shaking of intensity VI to VII, with large-scale mass transport becoming more frequent towards higher intensities (Monecke et al., 2004; Kremer et al., 2017). According to the Intensity Prediction Equation of Bakun and Wentworth (1997), a M_W 3.2 earthquake at 11 km distance would cause an intensity of IV$^{3}/_{4}$, while a M_W 3.9 earthquake at a distance of 23 km would cause an intensity of IV$^{1}/_{4}$. These intensities are thus below the thresholds for deformation structures found previously in Swiss lakes. However, Moernaut et al. (2014) observed delta failures at intensities of V½ in Chilean lakes, not much above the ground shaking intensities at Lake Biel in 1964 and 1965.

The strongest historical shaking at Lake Biel actually occurred during the earthquakes in Basel in 1356 (M_W 6.6) and Unterwalden (M_W 5.9), which affected the study area with an intensity of VII and VI, respectively (Fäh et al., 2003; Schwarz-Zanetti et al., 2003). However, no recent events are recorded that reached comparable intensities at Lake Biel. The fact that most recent failures (i.e. the orange MTD in the 1980s and the black MTD likely in 2000) happened without any significant registered earthquakes confirm the fact that lake slopes can fail without tremors, as seen for example in Lake Brienz in 1996 (Girardclos et al., 2007). In addition to earthquakes, natural factors that can trigger subaqueous mass transports include, among others, rock falls, flood events, gas charging, oversteepening and rapid sediment accumulation (e.g. Locat & Lee, 2002). Without an exact dating it is very hard to explore these possibilities, but historical data do not provide any indication that rock falls, flood events or gas charging may explain the orange and black mass transport events. In this case, the authors rather favour the various anthropogenic activities that are known to cause slope failures. For instance, the small-scale MTD located in front of Wingreis and Twann were most likely caused by construction works on the shoreline (Fig. 3A). In the case of Lake Biel, the deviation of the Aare River into the lake – in particular the concomitant increase in sediment delivery (Suppl. Mat.) leading to oversteepening and rapid sediment accumulation (Jeannet, 2012) – certainly played a key role in promoting the instability of the eastern shore, where most of the sediment is deposited (Weiss, 1977; Wright & Nydegger, 1980). The slopes in Lake Biel have thus been preconditioned since the Jura Water Corrections (JWC) and can fail both due to relatively small shaking intensities and also without trigger.

Wirth et al. (2011) already demonstrated such an increase in mass-movement occurrence following the deviation of the Kander River into Lake Thun in 1714. However, in the case of Lake Thun, sedimentation rates and mass-movement frequency decreased after 1840, as the Kander River adjusted to its previously lowered base level and the associated intense river channel erosion decreased. The Lake Thun sediment record contrasts with Lake Biel having frequent 20th Century mass transports and can be explained by two factors. First, the deviation of the Kander increased the river inflow into Lake Thun by (only) 60% whereas the deviation of the Aare into Lake Biel increased the inflow by a much higher 340% (from 55 to 240 m^3/s). In addition, the Kander deviation happened in 1714 and the natural river-lake interface was likely able to geomorphologically adjust during the next century to reach a new equilibrium around 1840. In contrast, the larger-scale JWC and the 1878 Aare deviation in Lake Biel (see above) combined both strong river inflow and artificial lake-level lowering. These particular sedimentological settings strongly increased the susceptibility of Lake Biel slopes to fail. Indeed, high-sedimentation lake slopes are known to fail without external trigger, as shown by the aseismic Muota delta collapse in 1687 (Hilbe & Anselmetti, 2014) or the large 1996 Aare delta collapse in Lake Brienz (Girardclos et al., 2007). Secondary effects of river engineering increasing sedimentation rate thus need to be taken into consideration, even though they might only increase sedimentological hazards after a latency of several decades due to threshold (i.e. sediment buildup) effects.

An additional and complementary explanation for the occurrence of the large 20th Century mass transports in deep Lake Biel is the dumping of materials excavated from the Nidau–Büren Channel during the second JWC, from 1963 to 1973 (Nast, 2006). The 2.7 million m^3 excavated material was transported on 300 m^3 hopper barges to an officially approved subaquatic disposal site located between Sutz–Lattrigen and Ipsach (Fig. 2), thus exactly where the large MTD complex is located. One exception is the washout of the 'sticky' lake chalk while the hopper barges were navigating, which left a distinctive whitish layer of lake chalk in many sediment cores from the central Tüscherz Basin (BIE-14-89, BIE-14-60, BIE-14-92, BIE-14-93, BIE-14-81, BIE-14-82, BIE-14-58 and BIE-14-83), also causing also a high amplitude seismic reflector close to the lake bed reflector.

The dumping of the excavated material at the disposal site was done in a water depth of *ca* 10 m; therefore most of the material must have been located on the slope. Many cores retrieved from the central part of the Tüscherz Basin, within or close to the MTD, reveal the presence of dumped material below 60 cm sediment depth (Fig. 4 pink circles; Fig. 6), such as sand lenses, angular stones (BIE-15-08) or grey clays (BIE-15-06). The distinction between dumped material and MTD is sometimes difficult, especially in the sediment cores from the yellow MTD (BIE-14-58, BIE-14-59, BIE-14-81 and BIE-14-82, Fig. 6). Thus, it is suggested here that the mass transports entrained background sediment but also the material dumped on the upper slope, which might have slid downslope with the rest of the sediments. This explains the great variety of sediment and the presence of conspicuous material in the cores in the MTDs. Given the location and the close timing, the dumping of the material excavated from the Nidau–Büren Channel could have also directly contributed to trigger the first and largest mass transport (yellow MTD, Fig. 4) and possibly the red MTD at the same time. The dumping started in 1963, while the yellow MTD was dated to the mid-1960s based on a turbidite (see *Dating the mass transports* section). Thus, sediment dumping, and its consequences for sediment stability, represent an additional secondary effect of river engineering that can lead to an increased sedimentological hazard. A likely more recent dump site can be observed from the multibeam data right in front of the Nidau–Büren Channel and results from the ongoing dredging of the channel (red bulge in Fig. 2).

In summary, three factors could have played a role in causing mass transports of the MTD complex: (i) sediment loading following the redirection of the Aare River into Lake Biel by the first JWC; (ii) dumping of material excavated from the Nidau–Büren Channel during the second JWC; or (iii) low magnitude earthquakes in 1964 and 1965 in the vicinity of Lake Biel (i.e. triggering the yellow MTD).

CONCLUSION

An integrated approach, combining subaqueous geomorphological mapping (multibeam echosounder data) with interpretation of reflection seismic profiles and analysis of sediment cores (including dating) was used to investigate the spatial and temporal distribution of recent mass transport structures in Lake Biel. In summary, Lake Biel reveals recurring cases of relatively large-scale subaquatic slope instabilities since the mid-1960s, likely caused by human interference in the 'Anthropocene'. Possible triggers of the observed mass transport complex (0.86 km^2) include low magnitude earthquakes, but the likely causes of the observed slope failures are the deviation of the Aare River and the accompanying dramatic increase in sediment delivery during the first Jura Water Corrections (JWC), as well as the subaquatic dumping of material excavated during the second JWC. The 2.7 million m^3 subaquatic landfill created by the second JWC dumping is clearly observable in sediment cores. The fact that it is likely linked to increased subaquatic slope instabilities questions the practice of sediment dumping that still occurs in lakes of the Swiss Plateau, and highlights the need for careful consideration of the location of dump sites.

Lacustrine subaqueous slope instabilities pose a risk for shore communities and infrastructures because various type of hazards are associated with mass transports: tsunamis (Schnellmann et al., 2006; Kremer et al., 2015; Hilbe & Anselmetti, 2015); collapse of shoreline (Kelts & Hsü, 1980); rupture of cables (see Pope et al., 2017, for a review) and blockage of a drinking water conduit as happened in December 2009 in Lake Biel (Råman Vinnå et al., 2017b). Therefore, large-scale river-management constructions such as the Jura Water Corrections need to consider possible short-term consequences of subaquatic landfills (i.e. sediment dumping), as well as longer-term effects, including the effects of higher sediment load on slope stability.

ACKNOWLEDGEMENTS

Initial research on the seismic reflection data and cores from Lake Biel was funded by the Swiss National Science Foundation (SNSF) projects 200021-121666 and 200020-146889. Funding for the bathymetric and LIDAR surveys was provided by the Swiss Federal Office of Topography (swisstopo), the Water and Waste Office Bern (AWA), the Federal Office for the Environment (FOEN), Energie Service Biel (ESB, Auftrag 5224001172), the Archeological Office Bern and the Water Restoration Fund Bern (Renaturierungsfonds). We are grateful to Irene Brunner and Alfred Lück for their help with sediment sampling and laboratory analyses, to Michael Strupler for help with MSCL and grain-size analyses, and to Adrian Gilli for access to the ETH Zurich Limnogeology Laboratory. We also thank Alois Zwyssig and Michael Schurter for sediment coring on Lake Biel, Katrina Kremer for help with the seismic profiling and fruitful discussions, Mischa Haas for modelling the sediment accumulation rate in BACON, Mathias Rüedi and Manuel Tièche from BASPO Ipsach (Swiss Federal Sport Office) for harbor logistics. The authors have no conflict of interest to declare. The data that support the findings of this study are available from the corresponding author upon reasonable request. We are also thankful to two reviewers, Maarten Van Daele and Emmanuel Chapron, who provided helpful comments that strengthened the final manuscript.

REFERENCES

Albrecht, A., Goudsmit, G., Zeh, M. (1999) Importance of lacustrine physical factors for the distribution of anthropogenic ^{60}Co in Lake Biel. *Limnol. Oceanogr.*, **44**, 196-206.

Albrecht, A., Reiser, R., Lück, A., Stoll, J.-M. A., Giger, W. (1998) Radiocesium Dating of Sediments from Lakes and Reservoirs of Different Hydrological Regimes. *Env. Sci. Technol.*, **32**, 1882-1887.

Amt für Wasser und Abfall (2015) Der neue Hagneckkanal: Besserer Hochwasserschutz, natürlichere Landschaft. AWA Fakten, Bern, 20 pp.

Anselmetti, F.S., Bühler, R., Finger, D., Girardclos, S., Lancini, A., Rellstab, C., Sturm, M. (2007) Effects of Alpine hydropower dams on particle transport and lacustrine sedimentation. *Aquat Sci,* **69**, 179–198.

Bakun, W.H. and **Wentworth, C.M. (**1997) Estimating earthquake location and magnitude from seismic intensity data. *Bulletin of the Seismological Society of America*, **87(6)**, 1502-1521.

Brombacher, C. (1997) Archaeobotanical investigations of Late Neolithic lakeshore settlements (Lake Biel, Switzerland). *Vegetation History and Archaeobotany,* **6(3)**, 167-186.

Cartigny, M.J.B., Postma, G., van den Berg, J.H., Mastbergen, D.R. (2011) A comparative study of sediment waves and cyclic steps based on geometries, internal structures and numerical modeling. *Mar. Geol.*, **280**, 40-56.

Chapron, E., Van Rensbergen,P., De Batist, M., Beck, C., Henriet, J.P. (2004) Fluid-escape features as a precursor of a large sublacustrine sediment slide in Lake Le Bourget, NW Alps, France. *Terra Nova*, **16(5)**, 305–311.

Chavaz, F. and **Gygax, S.** (1964) La IIe correction des Eaux du Jura. *Bulletin technique de la Suisse romande*, **9**, 173-184.

Cook, T. (2017) Damned if you do… They give us green energy but destroy precious river ecosystems. What can we do about dams, asks Terri Cook. *New Scientist,* **235 (3132)**, 36-39.

Covault, J.A., Kostic, S., Paull, C.K., Sylvester, Z., Fildani, A. (2017) Cyclic steps and related supercritical bedforms: building blocks of deep-water depositional systems, western North America. *Mar. Geol.,* **393**, 4-20.

Fäh, D., Giardini, D., Bay, F., Bernardi, F., Braunmiller, J., Deichmann, N., Furrer, M., Gantner, L., Gisler, M., Isenegger, D., Jimenez, M.J., Kästli, P., Koglin, R., Masciardi, V., Rutz, M., Scheidegger, C., Schibler, R., Schorlemmer, D., Schwarz- Zanetti, G., Steimen, S., Sellami, S., Wiemer, S., Wössner, J. (2003). Earthquake Catalogue of Switzerland (ECOS) and the related macroseismic database. *Eclogae Geol. Helv.,* **96 (2),** 219 – 236.

Fäh, D., Giardini, D., Kästli, P., Deichmann, N., Gisler, M., Schwarz-Zanetti, G., Alvarez-Rubio, S., Sellami, S., Edwards, B., Allmann, B., Bethmann, F., Wössner, J., Gassner-Stamm, G., Fritsche, S., Eberhard, D. (2011) ECOS-09 Earthquake Catalogue of Switzerland. Release 2011 Report and Database. Public catalogue, 17. 4. 2011. Swiss Seismological Service ETH Zurich, Report SED/RISK/R/001/20110417.

Gabbud, C., and **Lane, S.N.** (2016) Ecosystem impacts of Alpine water intakes for hydropower: the challenge of sediment management. *Wiley Interdisciplinary Reviews: Water,* **3(1)**, 41-61. DOI: 10.1002/wat2.1124.

Girardclos, S., Schmidt, O.T., Sturm, M., Ariztegui, D., Pugin, A., Anselmetti, F.S., (2007) The 1996 AD delta collapse and large turbidite in Lake Brienz. *Marine Geology,* **241**, 137-154.

Hilbe, M., and **Anselmetti, F.S.** (2014) Signatures of slope failures and river-delta collapses in a perialpine lake (Lake Lucerne, Switzerland). *Sedimentology,* **61**, 1883-1907.

Hilbe, M., and **Anselmetti, F.S.** (2015) Mass movement-induced tsunami Hazard on perialpine Lake Lucerne (Switzerland): Scenarios and numerical experiments. *Pure Appl. Geophys.* **172**, 545–568.

Jeannet, A. (2012) Lake Biel sediment record during the last 7500 years and impact of the Aare River deviation in 1878 AD, 82p. Maîtrise universitaire en sciences de l'environnement, Mémoire # 91, University of Geneva.

Kelts, K., and **Hsü, K. J.** (1980) Resedimented facies of 1875 Horgen slumps in Lake Zurich and a process model of longitudinal transport of turbidity currents. *Eclogae Geologicae Helvetiae*, **73(1)**, 271-281.

Kremer, K., Hilbe, M., Simpson, G., Decrouy, L., Wildi, W., Girardclos, S. (2015) Reconstructing 4000 years of mass movement and tsunami history in a deep peri-Alpine lake (Lake Geneva, France-Switzerland). *Sedimentology,* **62(5)**, 1305–1327. doi: 10.1111/sed.12190.

Kremer, K., Wirth, S.B., Reusch, A., Fäh, D., Bellwald, D., Anselmetti, F.S., Girardclos, S., Strasser, M. (2017), Lake-sediment based paleoseismology: Limitations and perspectives from the Swiss Alps, *Quaternary Science Reviews*, **168**, 1-18.

Ledoux, G., Lajeunesse, P., Chapron, E., St-Onge, G. (2010) Multibeam Bathymetry Investigations of Mass Movements in Lake Le Bourget (NW Alps, France) Using a Portable Platform. In D.C. Mosher et al. (eds.), Submarine Mass Movements and Their Consequences, *Advances in Natural and Technological Hazards Research*, **28**, 423-434.

Liechti, P. (1994) L'état des lacs en Suisse. Cahier de l'Environnement, 237. Office

Fédéral de l'Environnement, des Forêts et du Paysage (OFEFP), Berne, Suisse, 159 pp.

Locat, J., and **Lee, H.J.** (2002) Submarine landslides: advances and challenges. *Canadian Geotechnical Journal,* **39**, 193–212. doi: 10.1139/t01-089.

Moernaut, J., Daele, M. V., Heirman, K., Fontijn, K., Strasser, M., Pino, M., Urrutia, R., De Batist, M. (2014), Lacustrine turbidites as a tool for quantitative earthquake reconstruction: New evidence for a variable rupture mode in south central Chile. *J. Geophys. Res. Solid Earth*, **119**, 1607–1633.

Monecke, K., Anselmetti, F. S., Becker, A., Sturm, M., Giardini, D. (2004). The record of historic earthquakes in lake sediments of Central Switzerland. *Tectonophysics*, **394(1)**, 21-40.

Nast, M. (2006) Terre du lac, l'histoire de la correction des eaux du Jura. Verein Schlossmuseum Nidau. 200 pp.

Nydegger, P. (1967) Untersuchungen über Feinstofftransport in Flüssen und Seen, über Entstehung von Trübungshorizonten und zuflussbedingten Strömungen im Brienzersee und einige Vergleichsseen. *Beitr. Geol. Schwiez Hydrol. Ser.,* **16**, 92 pp.

Nydegger, P. (1976) Strömungen in Seen: Untersuchungen in situ und an nachgebildeten Modellseen. *Beitr. Geol. Schweiz. Kl. Mitt.,* **66**, 141-177.

Pope, E.L., Talling, P.J., Carter, L. (2017) Which earthquakes trigger damaging submarine mass movements: Insights from a global record of submarine cable breaks? *Marine Geology*, **384**, 131-146.

Praet, N., Moernaut, J., Van Daele, M., Boes, E., Haeussler, P.J., Strupler, M., Schmidt, S., Loso, M.G., De Batist, M. (2017) Paleoseismic potential of sublacustrine landslide records in a high-seismicity setting (south-central Alaska).

Marine Geology, **384**, 103-119.

Preusser, F., Reitner, J., Schlüchter, C. (2010) Distribution, geometry, age and origin of overdeepened valleys and basins in the Alps and their foreland. *Swiss Journal of Geosciences*, **103**, 407-426.

Råman Vinnå, L. (2018) Global and local anthropogenic effects on hydrodynamics of lakes applications to Lake Biel drinking water management, thesis no 7976, EPFL, Lausanne, DOI:10.5075/epfl-thesis-7976.

Råman Vinnå, L., Bouffard, D., Dubois, N., Hilbe, M., Käser, R., Wüest, A. (2017b) Seewasserentnahme im Bielersee. Gibt es eine ideale Position? *Aqua & Gas*, **97(9)**, 14-20.

Råman Vinnå, L., Wüest, A., Bouffard, D. (2017a) Physical effects of thermal pollution in lakes. *Water Resour. Res.*, **53(5)**, 3968–3987, doi:10.1002/2016WR019686.

Rayleigh, L. (1885) On waves propagated along the plane surface of an elastic solid. *Proceedings of the London Mathematical Society,* **17**, 4-11.

Reusch, A., Loher, M., Bouffard, D., Moernaut, J., Hellmich, F., Anselmetti, F.S., Bernasconi, S.M., Hilbe, M., Kopf, A., Lilley, M.D., Meinecke, G., Strasser, M. (2015) Giant lacustrine pockmarks with subaqueous groundwater discharge and subsurface sediment mobilization. *Geophysical Research Letters*, **42(9)**, 3465–3473, doi:10.1002/2015GL064179.

Santschi, P.W., and **Schindler, P.W.** (1977) Chemical and geochemical studies of Lake Biel I. A mass balance for Lake Biel and its implications for the rates of erosion of the drainage area. *Schweiz. Z. Hydrol.,* **39**, 182-200.

Schneider, J.R. (1881) Das Seeland der Westschweiz und die Korrektion seiner Gewässer. Krebs, Bern.

Schneider, N., Eugster, W., Schichler, B. (2004) The impact of historical land-use changes on the Near-Surface Atmospheric Conditions on the Swiss Plateau. *Earth Interactions*, **8(12)**, 1-27.

Schnellmann, M., Anselmetti, F.S., Giardini, D., McKenzie, J.A. (2006) 15,000 years of mass-movement history in Lake Lucerne: Implications for seismic and tsunami hazards. *Eclogae geol. Helv.,* **99**, 409–428.

Schnellmann, M., Anselmetti, F.S., Giardini, D., McKenzie, J.A. (2005) Mass movement-induced fold-and-thrust belt structures in unconsolidated sediments in Lake Lucerne (Switzerland). *Sedimentology.,* **52**, 271–289.

Schwarz-Zanetti, G., Deichmann, N., Fäh, D., Giardini, D., Jimenez, M.-J., Masciadri, V., Schibler, R., Schnellmann, M. (2003) The earthquake in Unterwalden on September 18, 1601: A historico-critical macroseismic evaluation. *Eclogae geol. Helv.*, **96**, 441-450.

Strupler, M., Hilbe, M., Anselmetti, F.S., Strasser, M. (2015) Das neue Tiefenmodell des Zürichsees: Hochauflösende Darstellung der geomorphodynamischen Ereignisse im tiefen Seebecken. *Swiss Bull angew Geo.,* **20,** 71–83.

Swisstopo (2014) Das hoch aufgelöste Terrainmodell der Schweiz. Detaillierte Produktinformation. Bundesamt für Landestopografie swisstopo, Wabern.

Symons, W.O., Sumner, E.J., Talling, P.J., Cartigny, M.J.B., Clare, M.A. (2016) Large-scale sediment waves and scours on the modern seafloor and their implications for the prevalence of supercritical flows. *Mar. Geol.,* **371**, 130-148.

Syvitski, J.P.M., Vörösmarty, C.J., Kettner, A.J., Green, P. (2005) Impact of humans on the flux of terrestrial sediment to the global coastal ocean. *Science*, **308(5720)**, 376-380.

Thevenon, F., Wirth, S.B., Fujak, M., Poté, J., Girardclos, S. (2013) Human impact on the transport of terrigenous and anthropogenic elements to peri-alpine lakes (Switzerland) over the last decades. *Aquat Sci*, **75**, 413–424.

Vischer, D.L. (2003) Histoire de la protection contre les crues en Suisse : Des origines jusqu'au 19e siècle. Rapports de l'OFEG, Série Eaux. No 5. Bienne. 208 p.

Vörösmarty, C.J., Meybeck, M., Fekete, B., Sharma, K., Greenand, P., Syvitski, J.P.M. (2003) Anthropogenic sediment retention: major global impact from registered river impoundments. *Global and Planetary Change,* **39**, 169 – 190.

Weiss, H.P. (1977) Sedimentologische und isotopengeochemische Untersuchung der Lockersedimente im Bielersee. 106p. Thesis, University of Bern.

Wessels, M., Anselmetti, F., Artuso, R., Baran, R., Daut, G., Gaide, S., Geiger, A., Groeneveld, J.D., Hilbe, M., Möst, K., Klauser, B., Niemann, S., Roschlaub, R., Steinbacher, F., Wintersteller, P., Zahn, E. (2015) Bathymetry of Lake Constance - A high-resolution survey in a large, deep lake. *ZFV - Zeitschrift für Geodäsie, Geoinformation und Landmanagement,* **140**, 203–210. doi: 10.12902/zfv-0079-2015.

Wirth, S.B., Girardclos, S., Rellstab, C., Anselmetti, F. (2011) The sedimentary response to a pioneer geo-engineering project: Tracking the Kander River deviation in the sediments of Lake Thun (Switzerland). *Sedimentology*, **58**, 1737–1761.

Wohlfarth, B. and **Schneider A.M.** (1991), Late Glacial and Holocene lake level fluctuations in Lake Biel, Western Switzerland. *Journal of Quaternary Science*, **6(4)**, 293-302.

Wright, R.F., and **Nydegger, P.** (1980), Sedimentation of detrital particulate matter in lakes: Influence of currents produced by inflowing rivers. *Water Resources Research*, **16**, 597-601.

Wright, R.F., Matter, A., Schweingruber, M., Siegenthaler, U. (1980), Sedimentation in Lake Biel, an eutrophic, hard-water lake in northwestern Switzerland. *Schweiz. Z. Hydrol.,* **42(2)**, 101–126.

Wüest, A., Zeh, M., Ackerman, J.D. (2007) Lake Brienz project: an interdisciplinary catchment-to-lake study. *Aquat Sci,* **69**, 173–178.

FIGURE CAPTIONS

Figure 1. Map of Lake Biel. (A) Location of Switzerland in Central Europe (B) Catchment of Lake Biel, before (hatched) and after (plain and hatched) the first Jura Water Correction (Swisstopo, 2014) (C) Map of the Seeland region showing Lake Biel, Lake Neuchâtel and Lake Murten, the various engineering work of the first and second Jura Water Corrections, as well as the locations of the 1964 and 1965 earthquakes (Swisstopo, 2014). The map is slightly tilted (see northward arrow).

Figure 2. Sublacustrine bathymetric map (shaded relief, colour indicating depth) of Lake Biel (top) with a hillshade map and interpretation of observed morphology (bottom). The four black rectangles (top) indicate the location of the geomorphological features highlighted in Fig. 3. The black star indicates the location of the long core, to the south-west of the Aare delta.

Figure 3. Selection of distinct geomorphological features observed in the high-resolution bathymetric data of Lake Biel: (A) small-scale mass transport deposit resulting from construction work on the shoreline; (B) channel incisions on the slope and mudflows; (C) pockmarks; and (D) subaquatic sand dunes. See Fig. 2 for location of these features.

Figure 4. Interpretation of the mass transport complex on a hillshade map. The locations of all the sediment cores retrieved are given in the small insert on the top left. Core analyzed in further detail are indicated with small black dots and their core names on the black and white hillshade map. Asterisks indicate dated cores.

The transverse seismic profiles T2 and T3 (Fig. 5) are shown by dotted lines. Outline of mudflows (grey) and mass transport deposits (colours by age as indicated on the figure) are provided. Locations, where excavated material was retrieved (at depth below 60 cm) are shown by pink circles. Cores in which turbidites were observed are underlined in green. Black stars represent cores in which a sand layer was present at 11 cm core depth. Yellow triangles (pointing down) represent cores in which lake chalk was present. Sediment creeping to the north-east of the mass transport complex is indicated with black arrows.

Figure 5. Seismic lines (A) and (B) along the longitudinal seismic profile (C) revealing the peculiar almost transparent unit across the entire Tüscherz Basin (SP = shot points, ms = milliseconds in two-way travel time). This transparent unit is thinning towards the shallower regions. The inset at the top left of panel (C) shows the location of the acquired 3.5 kHz seismic lines. The locations of the seismic lines (A), (B), (C), (D) and (E) are highlighted with thick red in the insert. The sediment surface in transverse line T1 (D) has a smoother topography than in transverse line T2 (E).

Figure 6. Cross cores correlation of the cores located – from left to right – outside of the mass transport complex, within the yellow MTD, orange MTD and red MTD as indicated by the colour bars on top (see Fig. 4 for locations). The numbers on top refer to the last two digits of the core number. Core BIE-14-61, which has been dated based on its ^{137}Cs activity profile (black ticks), is shown twice with ages indicated in the middle of the figure. The turbidite layers are bracketed in green. The black sand deposits are highlighted with dashed black vertical lenses. The beds interpreted as excavated material dumped in the lake are shown by pink vertical

lines or dashed pink vertical lines when mixed with background lacustrine sediment. Yellow triangles pointing down indicate the presence of lake chalk. The stars indicate the top of the mass transport deposits, with their colour corresponding to the respective MTD (see Fig. 4).

Figure 7. Dating of cores BL13-1C, BIE10-9 and BIE-14-61 based on their ^{137}Cs activity profile. BIE-14-62 was correlated with core BIE10-9 based on the two highlighted turbidites.

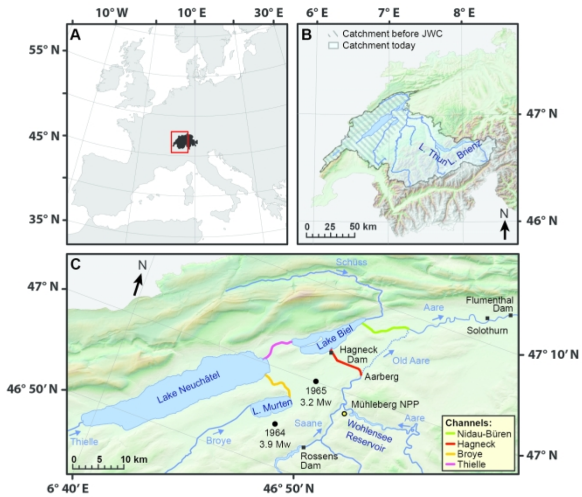

Figure 1. Location map of Lake Biel. (a) Location of Switzerland in Central Europe (b) Catchment of Lake Biel, before (hatched) and after (plain and hatched) the First Jura Water Correction (Swisstopo, 2014) (c) Map of the Seeland region showing Lake Biel, Lake Neuchâtel and Lake Murten, the various engineering work of the first and second Jura Water Correction, as well as the locations of the 1964 and 1965 earthquakes (Swisstopo, 2014). The map is slightly tilted (see northward arrow).

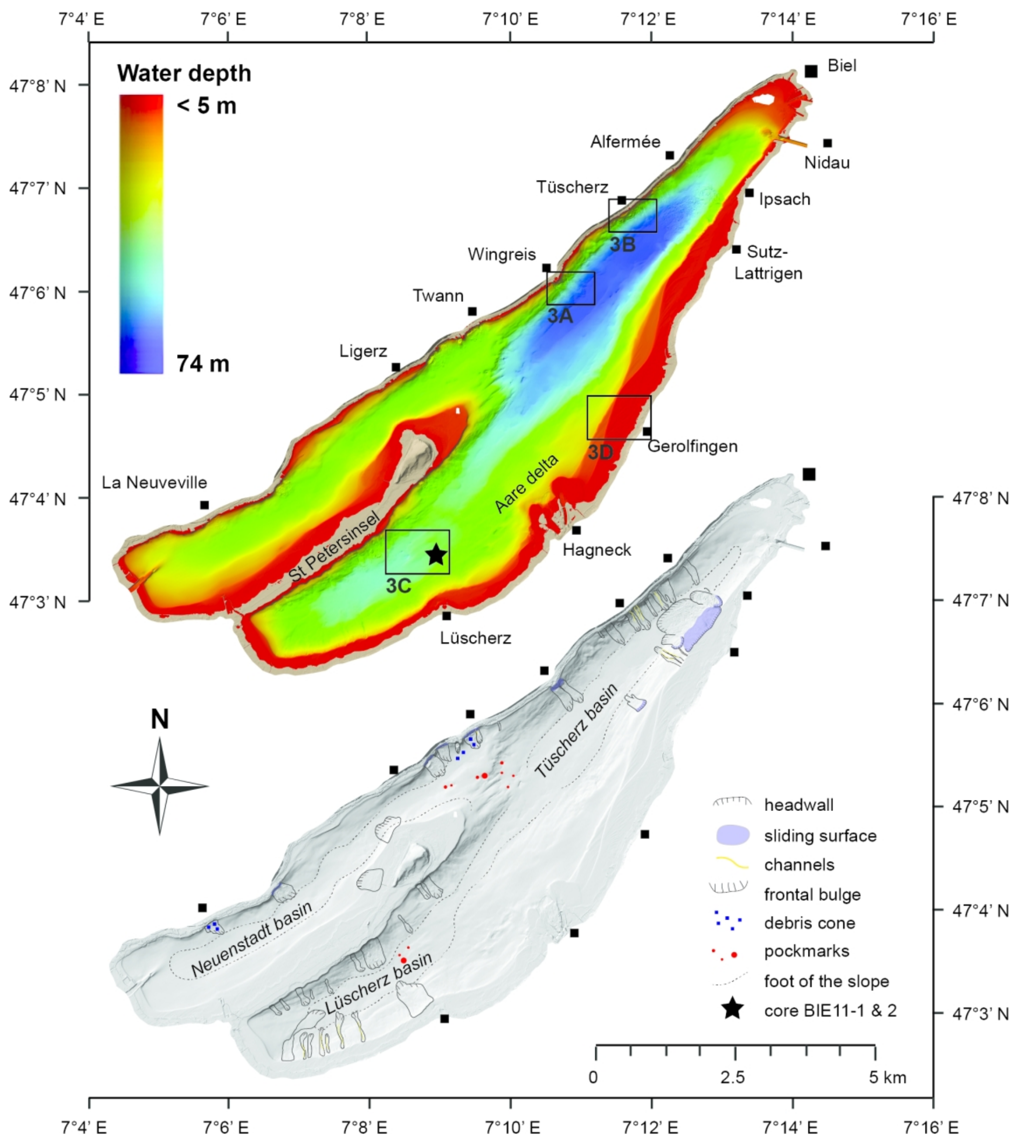

Figure 2. Sublacustrine bathymetric map (shaded relief, color indicating depth) of Lake Biel (top) with a hillshade map and interpretation of observed morphology (bottom). The four black rectangles (top) indicate the location of the geomorphological features highlighted in Figure 3. The black star indicates the location of the long core, to the southwest of the Aare delta.

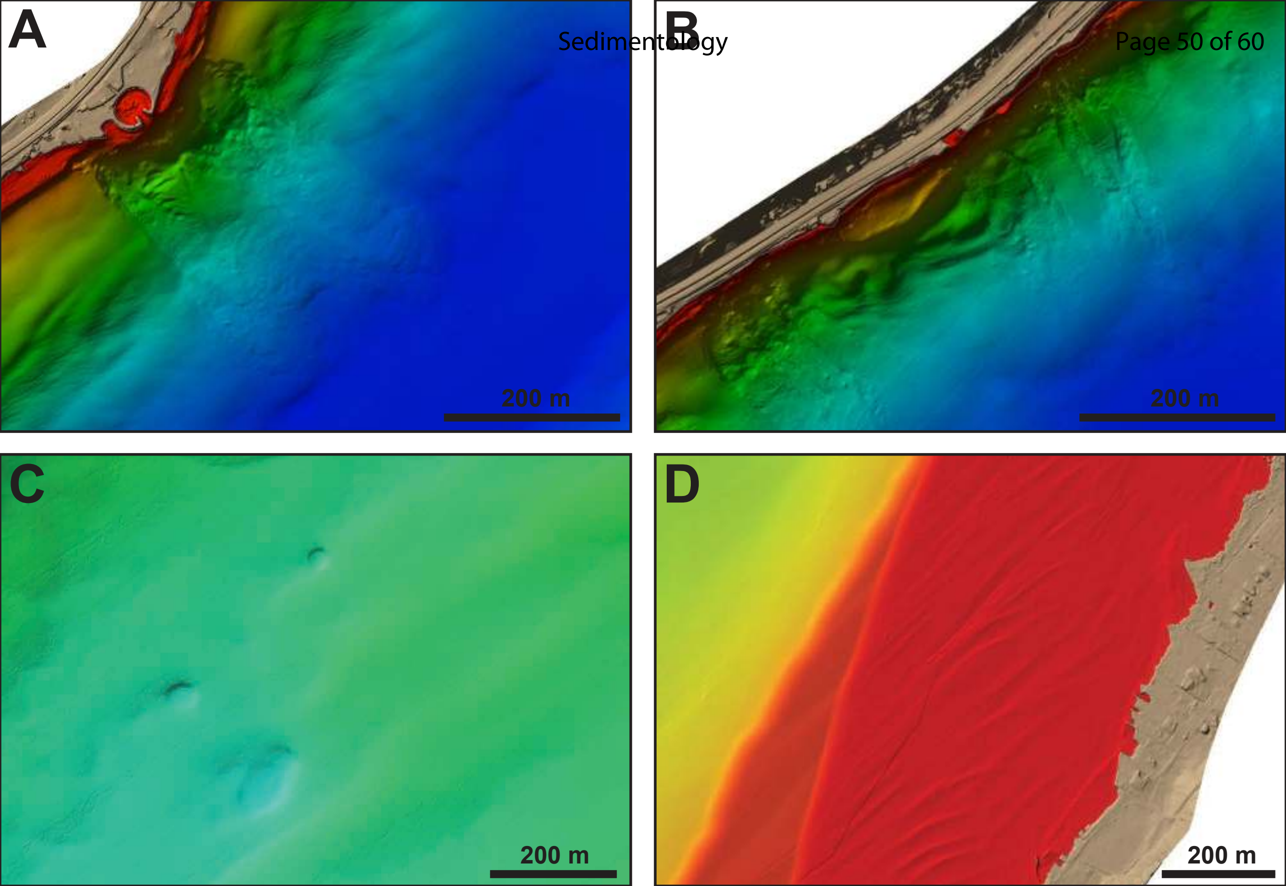
A
200 m
B
200 m
C
200 m
D
200 m

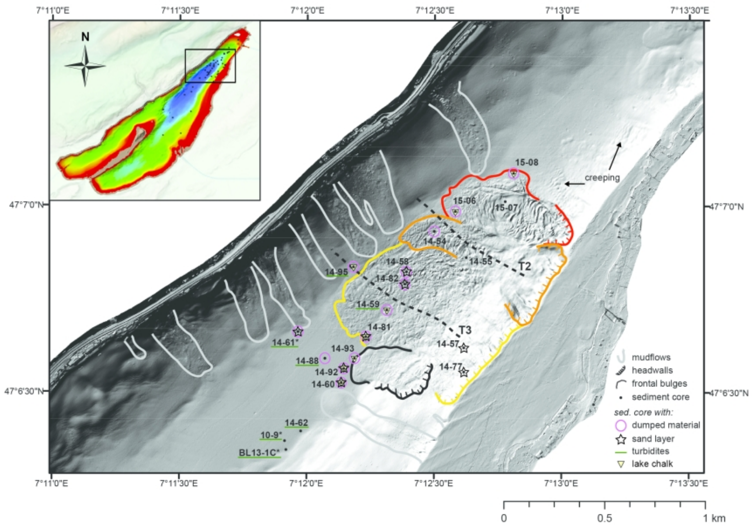

Figure 4. Interpretation of the mass-movement complex on a hillshade map. The locations of all the sediment cores retrieved are given in the small insert on the top left. Core analyzed in further detail are indicated with small black dots and their core names on the black and white hillshade map. Asterisks indicate dated cores. The transverse seismic profiles T2 and T3 (Fig.5) are shown by dotted lines. Outline of mudflows (grey) and mass transport deposits (colors by age as indicated on the figure) are provided. Locations, where excavated material was retrieved (at depth below 60 cm) are shown by pink circles. Cores in which turbidites were observed are underlined in green. Black stars represent cores in which a sand layer was present at 11 cm depth. Yellow triangles (pointing down) represent cores in which lake chalk was present. Sediment creeping to the northeast of the mass-movement complex is indicated with black arrows.

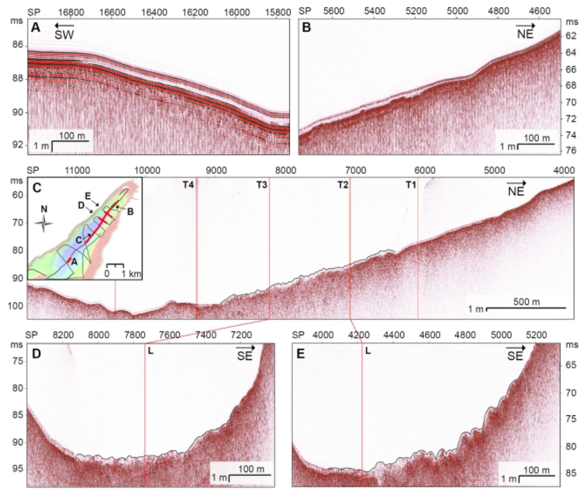

Figure 5. Seismic lines (A, B) along the longitudinal seismic profile (C) revealing the peculiar almost transparent unit across the entire Tüscherz basin (SP = shot points, ms = milliseconds in two-way travel time). This unit is thinning towards the shallower regions. The insert on the top left of panel C shows the location of the acquired 3.5 kHz seismic lines. The locations of the seismic lines (A, B, C, D, E) are highlighted with thick red in the insert. The sediment surface in transverse line T3 (D) has a smaller-scale topography than in transverse line T2 (E).

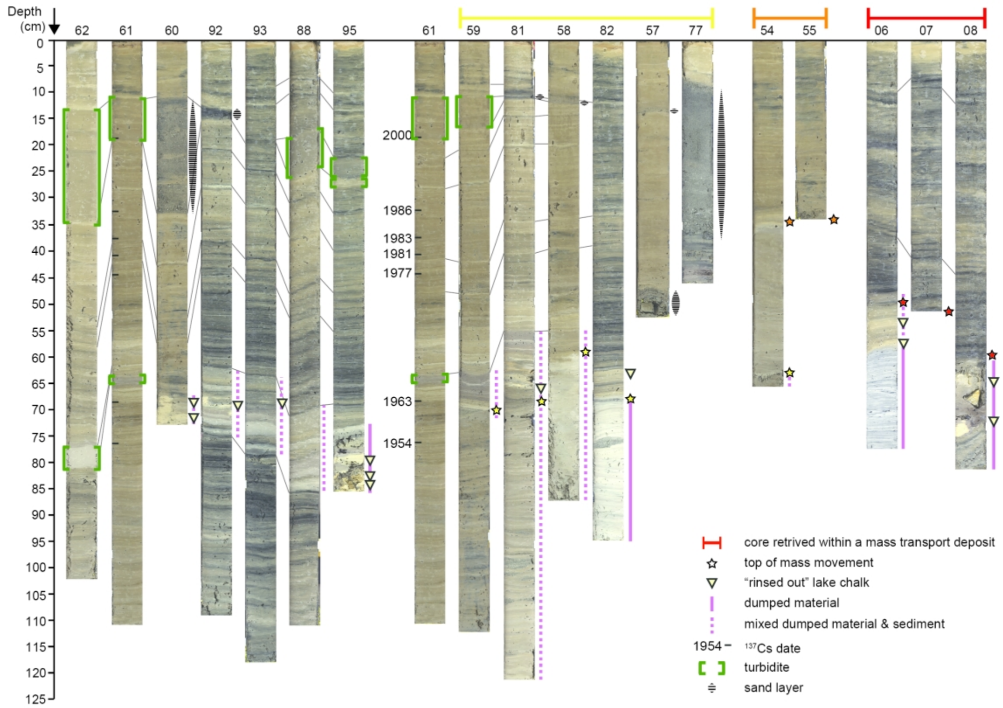

Figure 6. Cross cores correlation of the cores located -from left to right- outside of the mass-movement complex, within the yellow MTD, orange MTD and red MTD as indicated by the color bars on top (see Fig. 4 for locations). The numbers on top refer to last two digits of the core number. Core BIE-14-61, which has been dated based on its 137Cs activity profile (black ticks), is shown twice. 137Cs ages are only shown in next to the one in the middle of the figure. The turbidites are bracketed in green. The black sand deposits are highlighted with dashed black vertical lenses. The excavated material dumped in the lake is shown by pink vertical lines, or dashed pink vertical lines when mixed with background lacustrine sediment. Yellow triangles pointing down indicate the presence of lake chalk. The stars indicate the top of the mass movements, with their color corresponding to the MTD.

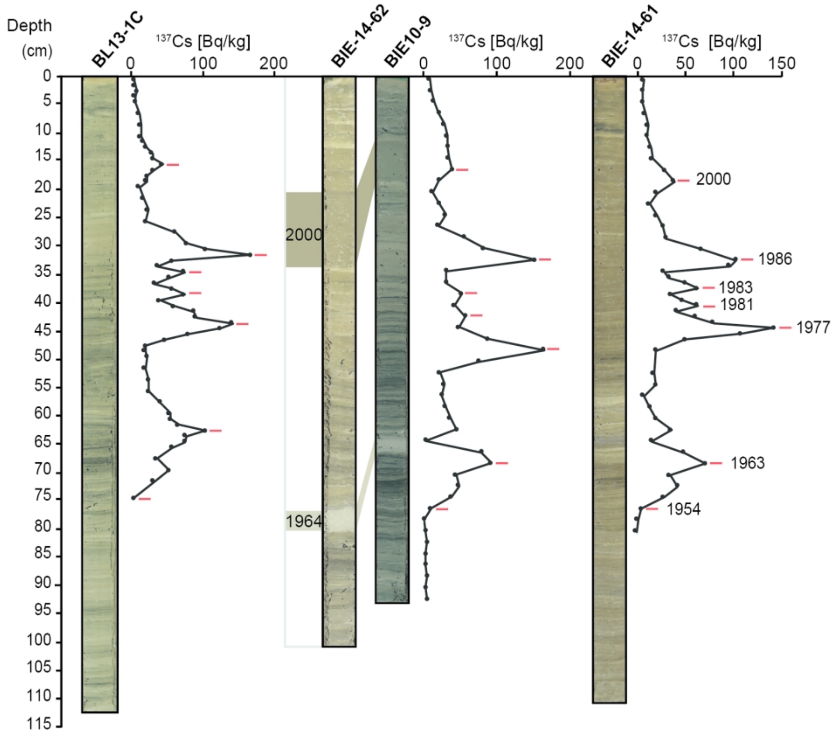

Figure 7. Dating of cores BL13-1C, BIE10-9 and BIE-14-61 based on their 137Cs activity profile. BIE-14-62 was correlated with core BIE10-9 based on the two turbidites highlighted.